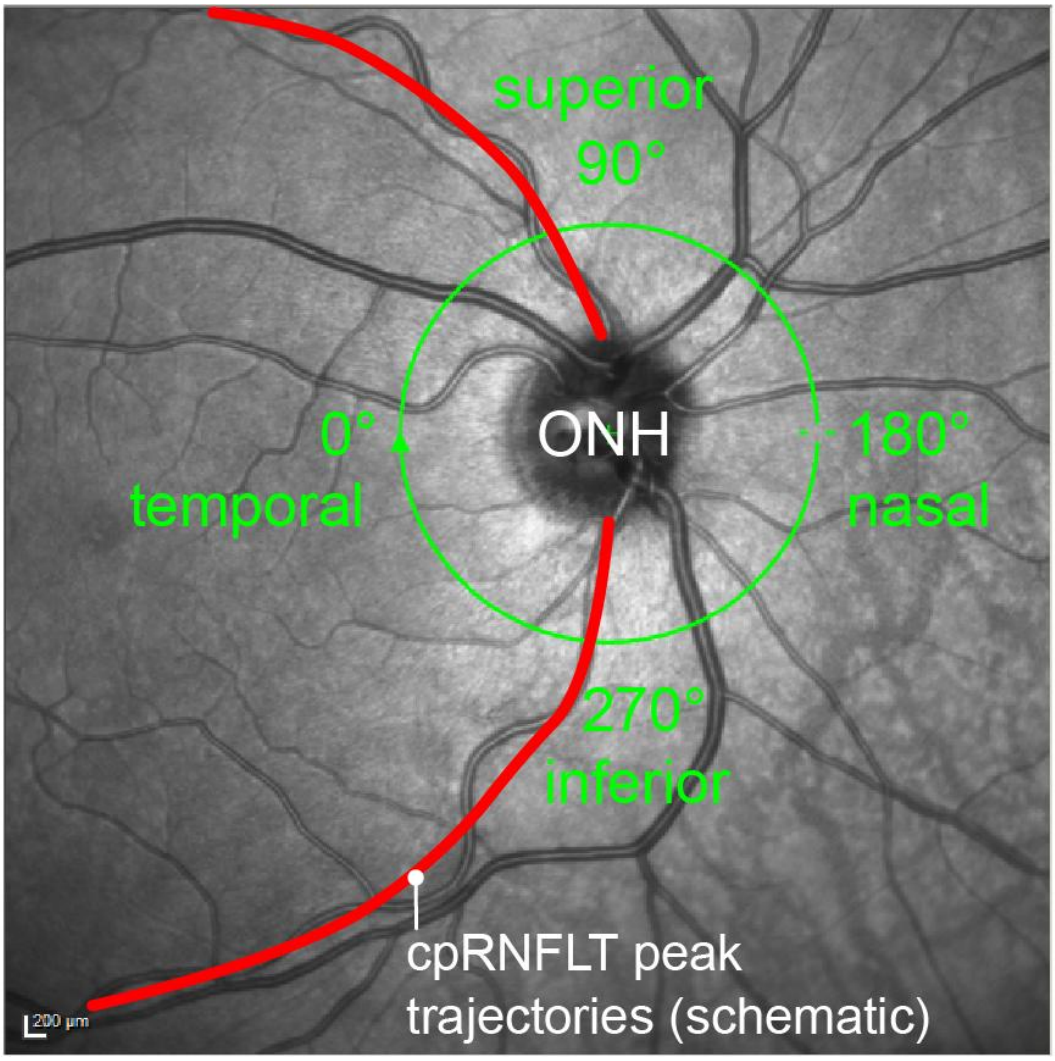

Figure S1

Retinal ganglion cell axons converge at the optic nerve head (ONH) and traverse the circumpapillary region. Measurement within this annular region therefore samples the entirety of retinal output, providing a comprehensive cross-sectional representation of all fibres conveying visual information to the brain.

Optical coherence tomography (OCT) was performed in order to obtain cpRNFLT scans with a resolution of 768 equidistant measurement points placed on a circle around the ONH. The location of the circle and its associated coordinate system are illustrated here. The thickest axon-rich bundles are the superior temporal and inferior temporal arcuate bundles, which form the 'double hump' in a normal cpRNFLT profile. The large retinal vessels (the superior temporal and inferior temporal arcades) run through these aformentioned sectors, meaning these cpRNFLT sectors are axon- and vessel-rich. In contrast, nasal sectors contain few major vessels and fewer macular axons, making them less axon- or vessel-rich compared with the superior temporal and inferior temporal peaks in cpRNFLT.

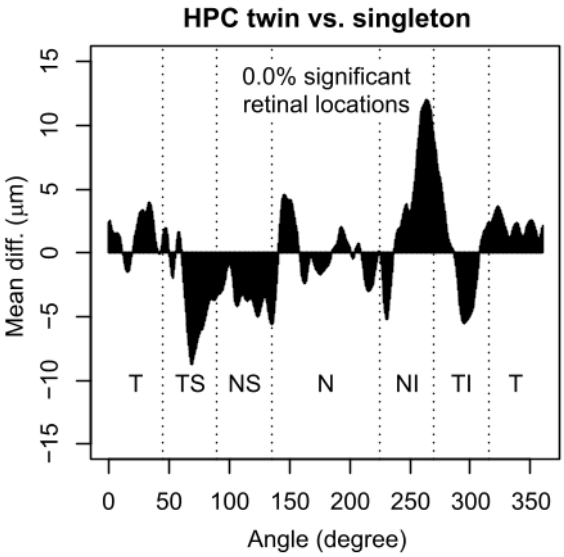

Figure S2

Figure S2 shows the subgroup analysis of differences in cpRNFLT (µm) for healthy twin pregnancies (n = 29) compared to healthy singleton pregnancies (HPC; n = 361). The plotted data comes from 768 individual points over 360° during the third trimester. The six standard sectors are plotted along the circular scan as follows: T (temporal, 315° to 45°), TS (temporal-superior, 45° to 90°), TI (temporal-inferior, 90° to 135°), N (nasal, 135° to 225°), NS (nasal-superior, 225° to 270°), and NI (nasal-inferior, 270° to 315°). Data was adjusted for refraction. Negative deflections on the y-axis are indicative of a reduction in the thickness of the nerve fibre layer in the aforementioned group compared to the latter group, while positive deflections are indicative of an increase. No statistically significant difference in retinal location was observed, possibly due to the limited number of cases included in the study. Nevertheless, twin pregnancies showed cpRNFLT thickening of approximately 12 µm between 240° and 280° in the NI sector, compared to HPC.

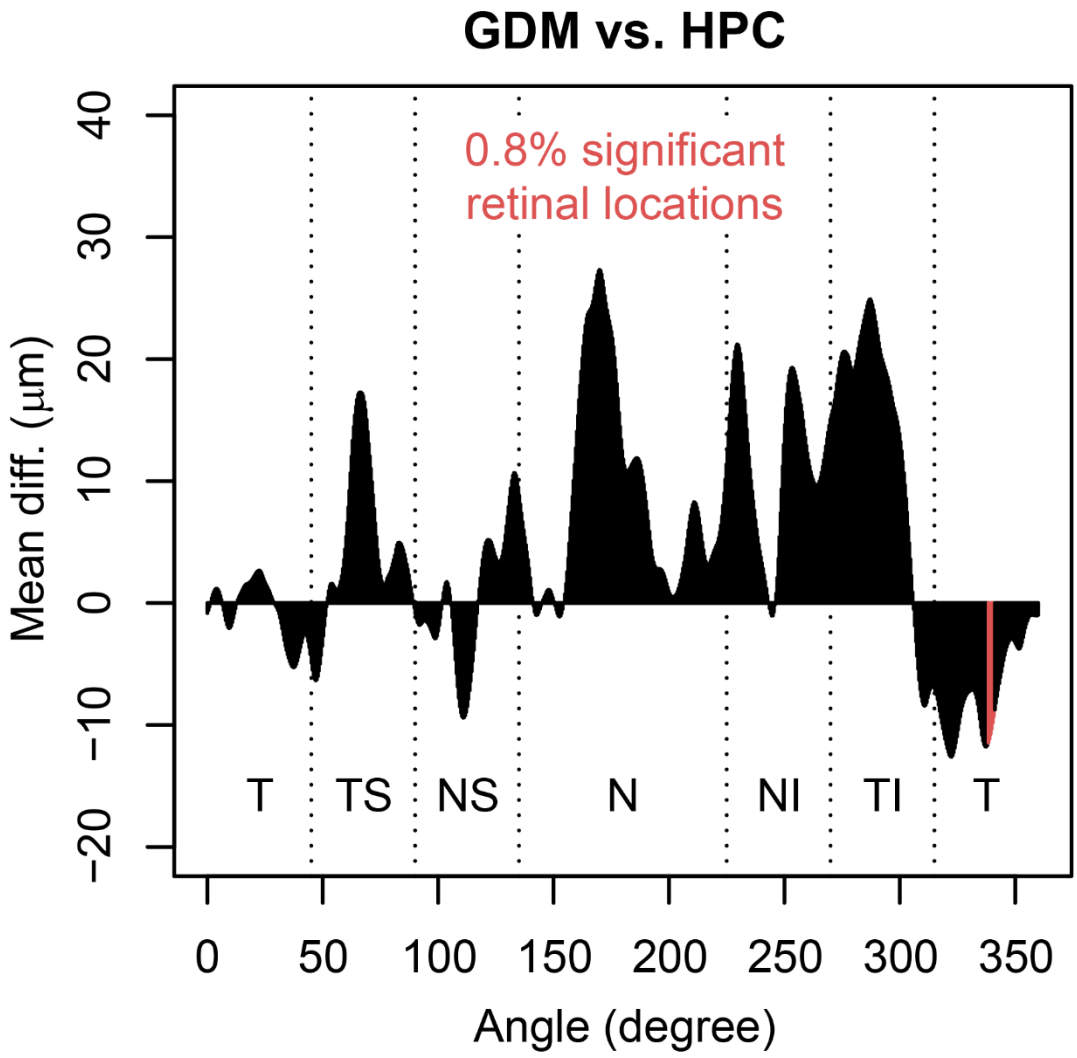

Figure S3

Figure S3 shows the subgroup analysis of differences in cpRNFLT (µm) for twin pregnancies with dGDM (n = 4) compared to healthy twin pregnancies (n = 29), plotted from 768 individual points over 360° in the third trimester. The six standard sectors are plotted along the circular scan as follows: T (temporal, 315° to 45°), TS (temporal-superior, 45° to 90°), TI (temporal-inferior, 90° to 135°), N (nasal, 135° to 225°), NS (nasal-superior, 225° to 270°), and NI (nasal-inferior, 270° to 315°). Data was adjusted for refraction. Negative deflections on the y-axis indicate thinning of the nerve fibre layer thickness in the aforementioned group compared to the latter group, while positive deflections indicate thickening. Areas of significant difference are indicated by a red colour scheme. Although only 0.8% of retinal locations differ significantly (i.e. due to the small sample size), the thickening between 225° and 300° and the thinning between 300° and 350° in the TI sector, as shown for the dGDM cohort of singleton pregnancies, were even more pronounced in twins.

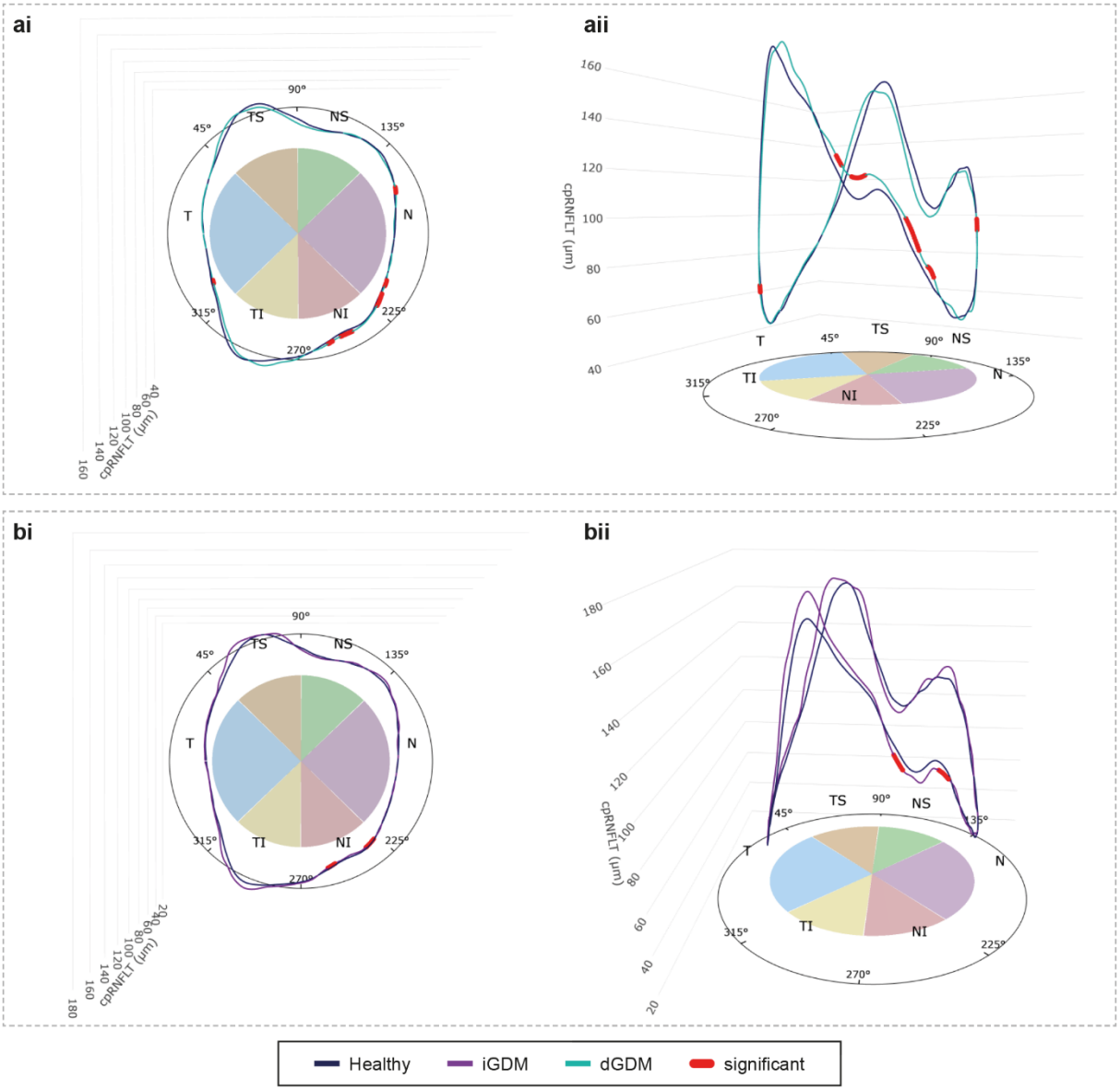

Figure S4

This visualization shows the differences in cpRNFLT at 768 A-scan locations on the circular scan for the Euclidean nested case-control matching of **Model 2** (matching for maternal age, gestational age at the time of measurement, refraction, systolic and diastolic blood pressure, and BMI at the time of examination and weight gain) between: **A**. Women with dGDM (n= 44, green); **B**. Women with iGDM (n= 21, purple) to their matched HPC (blue) in **i.** Bird's eye perspective and **ii**. three-dimensional (due to the high magnification and bird's-eye perspective, the circular scan appears more oval-shaped). Significant differences at the 768 individual measurement points ($p < .05$) are marked in red.

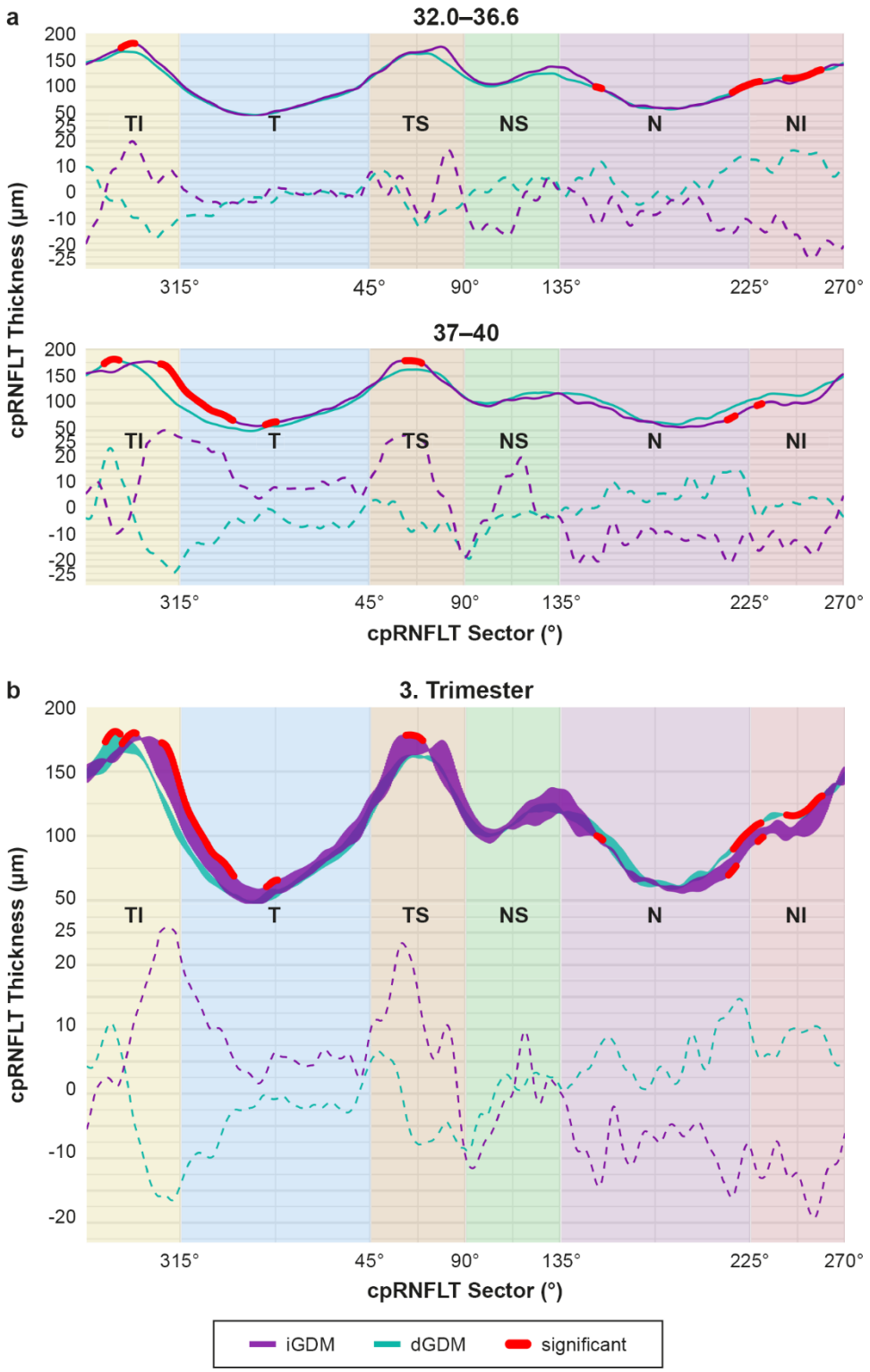

Figure S5

Figures S5A-B show the variation of the difference in cpRNFLT along the 768 individual A-scan measurement locations between dGDM (green) and iGDM (purple) versus HPC for different gestational age groups as well as the third trimester for **Model 2** of the Euclidean nested case-control approach.

In Figure S5B, plotted for gestational age within the 3rd trimester, the width of the shaded area between two depicted curves represents the change of cpRNFLT at the respective measurement location. Wider

shaded areas depict a larger evident change for the A-scan measurement region on the circular B-scan between 28.0 and 42.0 weeks of gestation. Narrow shaded areas depict stable cpRNFLT. Areas colored red indicate statistically significant differences ($p < .05$) for cpRNFLT of GDM to HPC. The graphs also represent the comparison between matched pairs for iGDM with HPC and matched dGDM with HPC. The dotted lines below indicate whether the differences in cpRNFLT mean thickening or thinning compared to the HPC. It should be noted that the data is only represented for weeks of gestation with sufficient measurement points to form matching pairs. Consequently, other data is not displayed.